Macrophages contribute to the pathogenesis of sclerosing cholangitis in mice

Maria Eugenia Guicciardi, Christy E. Trussoni, Anuradha Krishnan, Steven F. Bronk, Maria J. Lorenzo Pisarello, Steven P. O'Hara, Patrick L. Splinter, Yandong Gao, Pamela Vig, Alexander Revzin, Nicholas F. LaRusso, Gregory J. Gores

[1]Division of Gastroenterology and Hepatology and the Mayo Clinic Center for Cell Signaling in Gastroenterology (C-SiG), [2]Department of Physiology and Biomedical Engineering, Mayo Clinic, Rochester, MN, USA; [3]Allergan, South San Francisco, CA, USA

Table of contents

Materials and methods

Reagents. The IAP antagonist BV6 was purchased from Selleck Chemical (Houston, TX). Lipopolysaccharide (LPS) from *E.coli* was purchased from InvivoGen (tlrl-3pelps; San Diego, CA). Neutralizing antibodies against human IL-6 (MAB2061R), human IL-8/CXCR2 (MAB331), and human CCL2/MCP1 (MAB279) were purchased from R&D Systems (Minneapolis, MN). Cenicriviroc (CVC) was a generous gift from Allergan (South San Francisco, CA). All other reagents were from Sigma Aldrich (St. Louis, MO), unless otherwise specified.

Cell lines. The SV40-transformed, non-malignant human cholangiocyte cell line H69 (obtained from Dr. G.Jefferson, Tufts University, Boston, MA), and low-passage (passage 16), spontaneously immortalized normal human cholangiocytes (NHC, obtained from Dr. Juan Medina, University Hospital, Pamplona, Spain) were grown as previously described.[1-3] PSC patient-derived cholangiocytes (passage 4), isolated from patients with stage 4 PSC without cholangiocarcinoma, were obtained, cultured and characterized as previously described. The cells expressed cholangiocyte (cytokeratin 7 and 19) and epithelial cell adhesion markers (EpCAM, ICAM) and still retained phenotypic characteristics of disease as assessed by beta galactosidase staining for senescence and ELISA assessment of increased secretion of SASP markers.[4] The human monocytic cell line THP-1 was obtained from ATCC (Manassas, VA; TIB-202), and cultured as previously described.[5] All cell lines were tested for absence of mycoplasma contamination (MycoAlert™ mycoplasma detection kit, Lonza, Basel, Switzerland) and authenticated by Short Tandem Repeat (STR) analysis.

Histological analysis. Thirty-one liver tissue specimens consisting of three stage 1, three stage 2, and three stage 3 PSC from needle biopsies, fourteen stage 4 (cirrhotic stage) PSC with no evidence of cholangiocarcinoma from liver explants, and eight normal liver tissue specimens from biopsies of patients undergoing bariatric surgery were used. Four primary biliary cholangitis (PBC) and hepatitis C (HCV) tissue samples were obtained from liver explants from stage 4 patients for both diseases. Liver samples were collected with Institutional Review Board approval.

For immunohistochemistry, human and mouse liver tissues were processed as previously described[6] and incubated overnight with primary antibodies against CD68 (1:200), or PanCK (1:1000)(Supplementary CTAT Table). Bound antibodies were detected with either biotin conjugated (Vector Laboratories, Burlingame, CA) or HRP conjugated secondary antibodies (Dako, Carpinteria, CA) using diaminobenzidine tetrahydrochoride as chromogen. Tissue slices were counterstained with hematoxylin. Hematoxylin/eosin stain was performed by standard methods. Liver fibrosis was examined using Picrosirius red staining as previously described[7]. Images were obtained using a Nikon Eclipse TE300 microscope (Nikon, Tokyo, Japan) equipped with Nikon Digital Sight DS-Ri1. Parenchymal and peribiliary macrophages ($CD68^+$) quantification was performed using the NIS Elements AR 4.60 imaging software (Nikon). The peribiliary area was defined as 50-60 μm from the basement membrane and manually determined using the image's scale bar.

For immunofluorescence, human and mouse formalin-fixed, paraffin-embedded liver tissue sections were deparaffinized, rehydrated, and exposed to heat-mediated antigen retrieval in low-pH antigen unmasking solution (Vector Labs, Burlingame, CA). Tissue sections were subsequently treated with Image-iT FX Signal Enhancer (Thermo Fisher Scientific, Waltham,

MA) and incubated in blocking buffer (10% normal serum, 1% bovine serum albumin, 0.1% Triton-X 100 in PBS) for 1 hour at room temperature. Tissue sections were then incubated overnight at 4°C with the following primary antibodies (Supplementary CTAT Table): anti-human/mouse CD68 (Abcam, 1:250), anti-human CD206 (R&D Systems, 1:100), anti-mouse CD206 (R&D Systems, 1:100), anti-human/mouse iNOS (Abcam, 1:100), anti-human/mouse iNOS (R&D Systems, 1:50), anti-human CCR2 (R&D Systems, 1:50), anti-mouse CCR2 (Novus Bio, 1:50), anti-mouse Clec4F (R&D Systems, 1:100); anti-human/mouse CK19 (Santa Cruz Biotech., 1:50), anti-human/mouse CK19 (Abcam, 1:100); anti-human/mouse EpCAM (Abcam, 1:100). Negative control images were generated using isotype controls (Supplementary CTAT Table) at the same concentrations as the respective primary antibodies and are provided in Suppl. Fig. S6. Tissue sections were subsequently incubated for 1 hour at room temperature with Alexa-Fluor secondary antibodies (Supplementary CTAT Table; 1:200), and mounted in Prolong Gold Antifade with DAPI (Thermo Fisher Scientific). Slides were allowed to dry and then imaged on a Zeiss 710 confocal microscope (Oberkochen, Germany). Peribiliary macrophages were quantitated by manually counting the number of $CD68^+$ cells within the peribiliary area as defined above.

Next generation sequencing (NGS). Gene expression profile in normal cholangiocyte cell lines and PSC patient-derived cholangiocytes was analyzed by next generation sequencing as previously described[4].

Enzyme-linked immunosorbant assay (ELISA). Conditioned media were obtained as described above and stored at -80˚C until used. Human IL-6, IL-8, CCL2/MCP-1 and CCL20 (D5060, D8000C, DCP00, DM3A00; R&D Systems), CXCL2 (Ab184862, Abcam), and CXCL3 (LS-F11251-1, Lifespan Biosciences, Seattle, WA) in the supernatants were measured using

ELISA kits following the manufacturer's instructions. Each assay was performed in duplicate on samples obtained from three separate experiments in triplicate. Conditioned media were obtained as described above.

Macrophage migration assays. H69, NHC, and PSC-derived cholangiocytes were plated in equal number in 6-well plates and cultured for 24 hr in complete medium. After this time, H69 and NHC reached approx. 80% confluence, whereas PSC/senescent cells grow at a slower pace, therefore their number was lower at the time of collection of the condition media compared to controls; however, PSC/senescent cells are hypersecretory, therefore we used the same volume of conditioned media (1 ml, undiluted) for all subsequent assays. H69 cells were treated with DMEM + 2% FBS with or without BV6 (5 μM) for 1 hour, then washed with PBS and incubated in DMEM + 2% FBS for 23 hours. PSC-derived cholangiocytes were cultured DMEM + 10% FBS for 24 hours. The conditioned medium was then removed, centrifuged at 3,000 *x g* for 15 min and transferred to the receiver wells of a Cell Biolabs CytoSelect™ 96-well Cell Migration Assay Kit equipped with a polycarbonate membrane plate (5 μm pore size; Cell Biolabs Inc., San Diego, CA). Twenty four-hour conditioned media from normal human cholangiocytes (NHC) treated with LPS for 10 days (experimentally-induced senescent cholangiocytes) was used as positive control and DMEM + 10% FBS was used as negative control. In a subset of experiments, neutralizing antibodies against IL-8 (2.5 μg/ml) or CCL2 (2.5 μg/ml) were added to the conditioned media. THP-1 cells were pre-incubated in serum-free DMEM for 1 hour, then resuspended in either DMEM + 2% FBS (for BV6-conditioned media experiments) or DMEM + 10% FBS (for PSC conditioned media experiments) and plated into the upper chamber of the 96-well plate at a concentration of 2 x 10^5 cells/100μl/well. After 6 hours, cells migrating through the membrane and attached to the bottom side were dissociated from the membrane, lysed and

quantified using the DNA-binding CyQuant® GR fluorescent dye and a fluorescence plate reader at 480 nm/520 nm.

Selected experiments were performed employing static microfluidic co-culture devices fabricated as previously reported.[8] Briefly, dual-chamber microfluidic devices measuring 75 μm in height with microgrooves (100 μm in length, 5 μm in height, 10 μm in width) separating the parallel chambers were used. The microfluidic platforms were first coated with a collagen I solution (0.2 mg/ml) for 4 hours at 37°C in a cell incubator. NHC or PSC-derived cholangiocytes were seeded at a density of 2 x 10^6 cells/ml in one chamber of the device and allowed to grow in culture, whereas the second chamber was filled with culture media alone. After 48 hours, the growth media was removed and replaced with RPMI containing 10% fetal bovine serum, with or without neutralizing antibodies against IL-8 or CCL2. At this time THP-1 cells, previously stained with CellTracker Red CMTPX dye (C34552, ThermoFisher Scientific) for 1 hour, were plated in the second chamber at a density of 2 x 10^6 cells/ml. Images of the THP-1 cells were taken on a fluorescence microscope (Nikon Eclipse TE300, Nikon, Tokyo, Japan) immediately after the cells settled (~30 min, set as time 0) and after a 24 hour incubation in the chamber, and the number of THP-1 cells that migrated through the grooves into the chamber containing NHC or PSC cells was quantitated.

Macrophage activation assay. THP-1 cells were resuspended in serum-free DMEM and plated in equal number in 6-well plates (approx. 5 x 10^5 cells/well). After 2 hr., when the most of the cells have adhered to the bottom of the plate, the medium was replaced with conditioned medium (1 ml) obtained from H69 cells with/without BV6 treatment, NHC, PSC-derived cholangiocytes (from two patients) and LPS-treated NHC as described above. In a subset of experiments, neutralizing antibodies against IL-6 (0.5 μg/ml), IL-8 or CCL2 were added to the

conditioned media. Total RNA was collected after 6 hr and analyzed by RT-qPCR for markers of activation (*IL6* and *IL1β*) using the primers listed in Supplemental CTAT table.

Hydroxyproline assay. Hydroxyproline assay as a direct measurement of collagen content was performed on frozen liver specimens (100 mg) as described before. [9]

Serum analysis. Serum alanine aminotransferase (ALT), total bile acids and total bilirubin were measured using a commercially available veterinary chemistry analyzer (VetScan 2, Abaxis, Union City, CA).

Reverse transcription-quantitative polymerase chain reaction (RT-qPCR). Total RNA extraction was performed using RNeasy® Plus mini kit (Qiagen, Hilden, Germay). RT was performed starting from 1 μg of total RNA as previously described.[6] qPCR was performed in a total volume of 10 μl containing 10 ng cDNA/reaction, at the following cycling conditions: 95°C for 5 min (activation); 95°C for 10 seconds, 60°C for 10 seconds, 72°C for 30 seconds (40 cycles, amplification); 95°C for 5 seconds, 65 C for 1 min, followed by dissociation curve analysis. Primers used are listed in Supplemental CTAT Table. Target gene expression was calculated using the ΔΔCt method and expression was normalized to GAPDH (human cells) or hypoxanthine-guanine phosphoribosyltransferase (HPRT; mouse tissue) expression levels.

Flow cytometry. Liver tissue obtained from experimental animals described above was enzyme dissociated as per manufacturer's protocol using the gentleMACS dissociator (Miltenyi Biotech, Somerville, MA). Whole cell isolates were subjected to red cell lysis using ACK buffer. Total cell number was counted on a cell counter (Cellometer®, Nexcelom Bioscience, Lawrence, MA) and 5 x 10^6 cells were used to label with CD45-conjugated TIL microbeads for separation on a magnetic column (Miltenyi Biotech). $CD45^+$ leucocytes were stained with fluorochrome-conjugated antibodies against CD45 (REA737-Viogreen), F4/80 (REA126-PE),

CD11b (REA592-PerCP Vio700), Ly6C (REA796-APC-Vio770), CCR2 (REA538-PE), and CD3 (REA641-FITC) (Miltenyi Biotech) and analyzed for multicolor flow cytometry on MACSQUANT Analyzer 10 (Miltenyi Biotech) using appropriate FMO (fluorescence minus one) controls. The Vioblue dye (Miltenyi Biotech) was used to sort live from dead cells. Gating strategy and FMOs are illustrated in Suppl. Fig. S7. Data were analyzed on Flow Logic v7.2 (Inivai, Victoria, Australia).

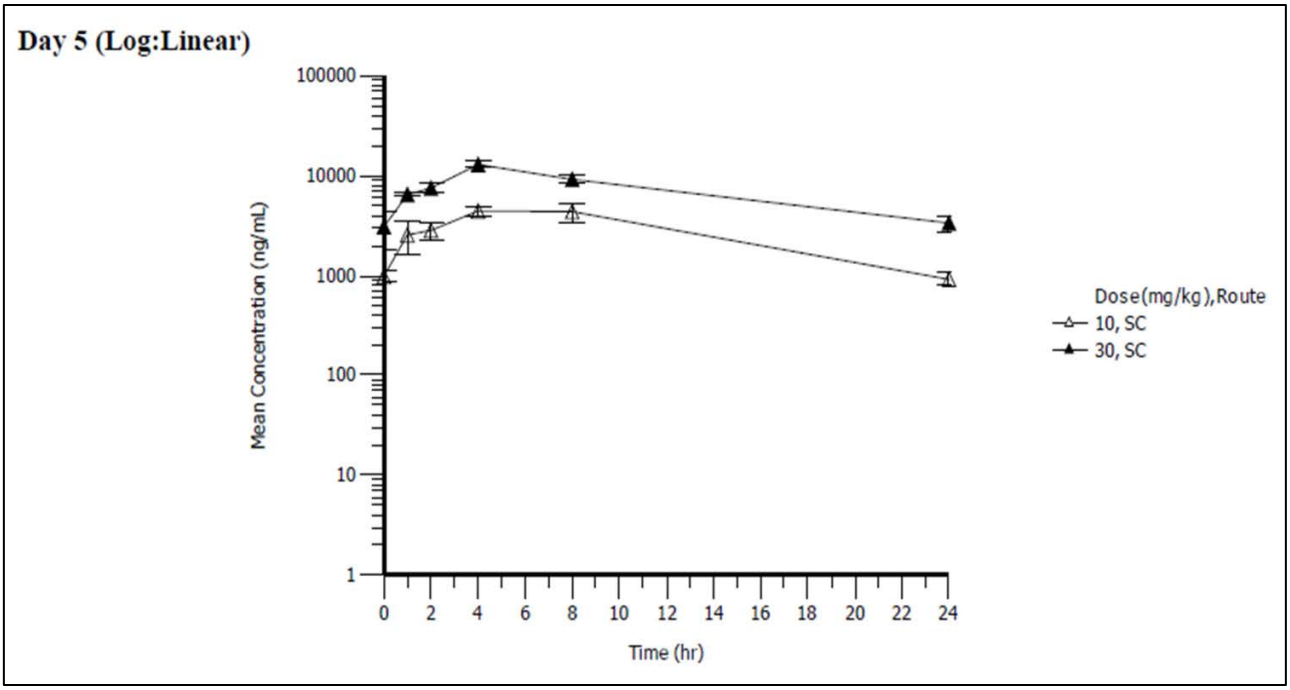

Fig. S1. Cenicriviroc (CVC) plasma concentration-time profiles on Day 5 following subcutaneous administration of 10 and 30 mg/kg CVC to male mice. Data expressed as mean ± SD of CVC plasma concentrations on Day 5 following daily subcutaneous (SC) administration of 10 and 30 mg/kg CVC, measured at 0, 1, 2, 4, 8 and 24 hr. after last dose (n=3/time point).

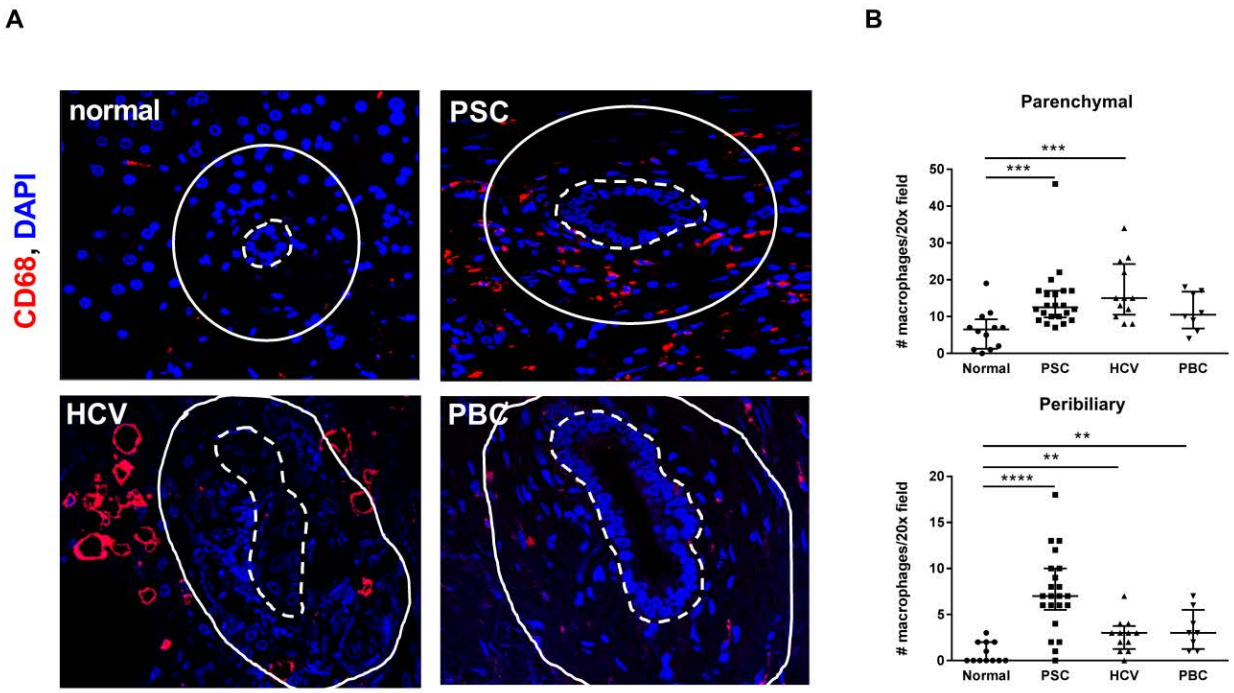

Fig. S2. Peribiliary accumulation of macrophages is greater in primary sclerosing cholangitis (PSC) compared to other liver diseases. (A) CD68 immunofluorescence on the liver of patients with stage 4 PSC, primary biliary cholangitis (PBC), hepatitis C (HCV) and normal livers. 20x magnification. The dotted lines indicate the bile ducts; the solid lines indicate the analyzed peribiliary area. **(B)** Quantification of $CD68^{+}$ parenchymal and peribiliary areas (n=4 per group, multiple fields assessed).

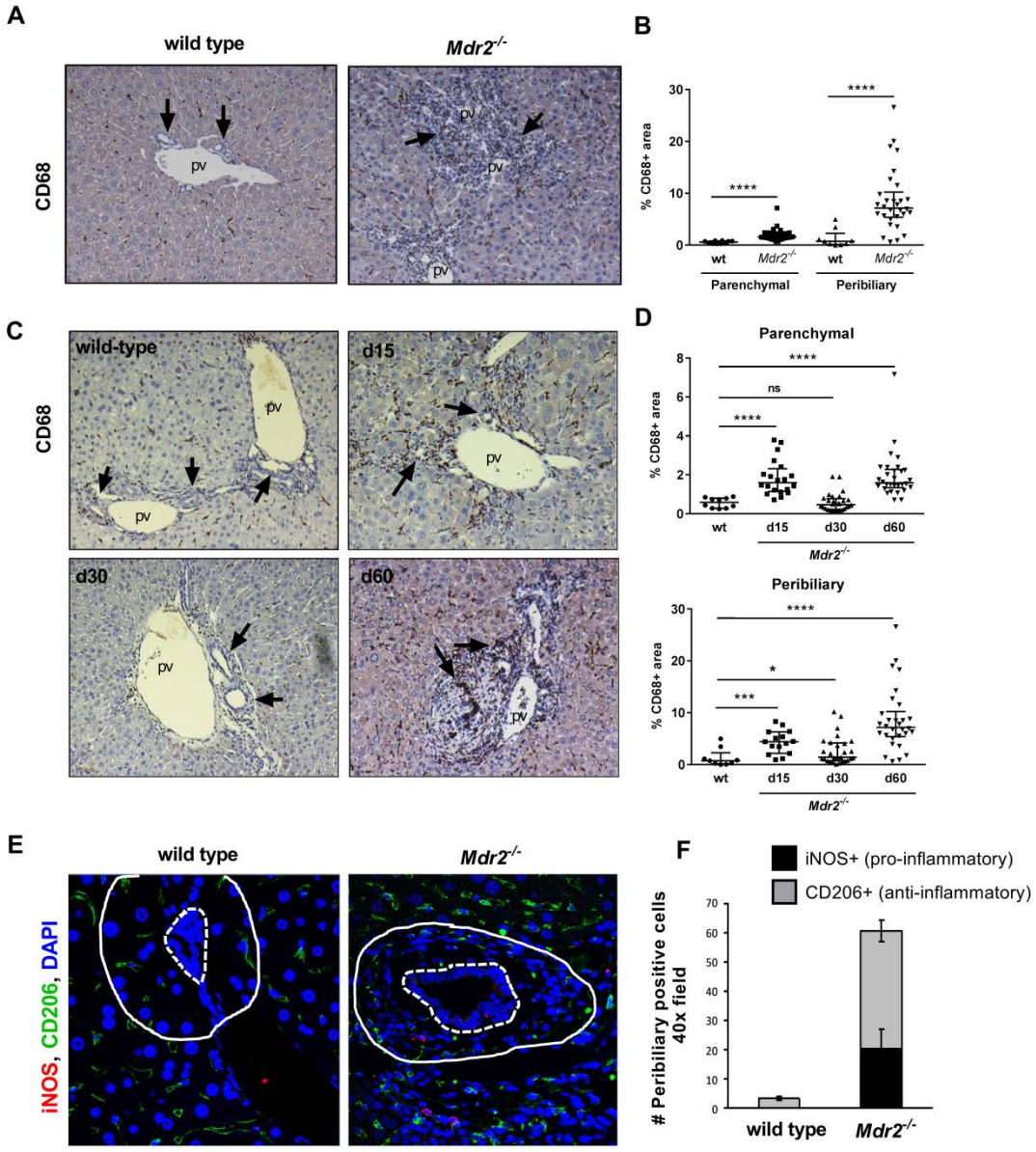

Fig. S3. Macrophages accumulate in the peribiliary areas of FVB.*Mdr2*$^{-/-}$ mouse livers. (A) CD68 immunohistochemistry on liver sections from sixty-day old wild-type and FVB.*Mdr2*$^{-/-}$ mice; 10x magnification. **(B)** Quantification of CD68+ parenchymal and peribiliary areas (wt: n=1 male, 1 female; *Mdr2*$^{-/-}$: n=5 males, 1 female). **(C)** Representative CD68 immunohistochemistry on liver sections from wild-type and 15-, 30- and 60-days old FVB.*Mdr2*$^{-/-}$ mice; 20x magnification. **(D)** Quantification of CD68-positive parenchymal and peribiliary areas (wt: n= 1 male, 1 female; d15: n= 4 males; d30: n= 3 males, 3 females; d60: 5 males, 1 female). **(E)** Representative iNOS and CD206 co-immunofluorescence on liver tissue of sixty-day old wild-type and FVB.*Mdr2*$^{-/-}$ mice. The dotted line indicates the bile duct; solid line indicates the analyzed peribiliary area. **(F)** Quantification of iNOS^{+} and CD206^{+} peribiliary cells (wt: n= 3 females; *Mdr2-/-*: n= 2 males, 1 female). **p<0.05.

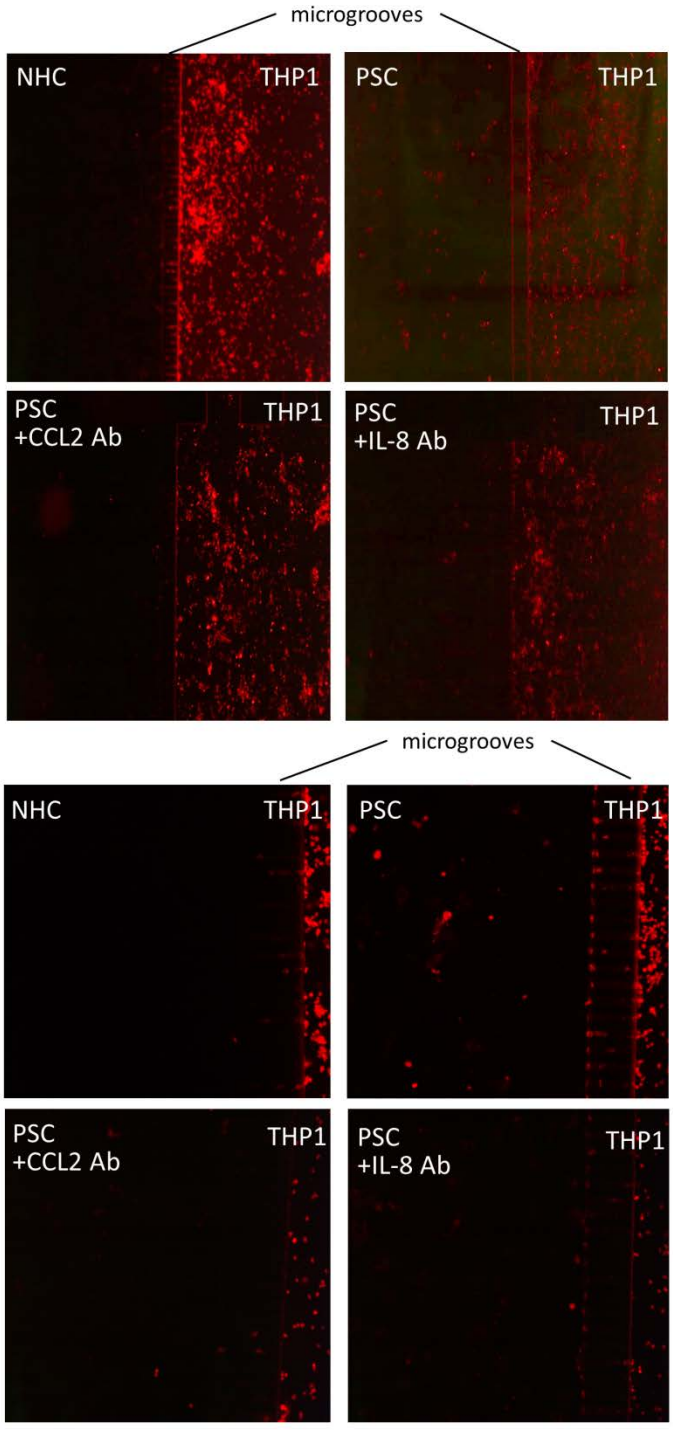

Fig. S4. THP-1 migration assay in response to diseased cholangiocyte-released chemokines. Unstained NHC (control) or PSC cholangiocytes were seeded in one chamber of a microfluidic device. After 48 hr. the medium was replaced with fresh RPMI ± neutralizing antibodies against CCL2 or IL-8, and THP-1 cells (red) were plated in the adjacent chamber. Migration of THP-1 cells through the microgrooves separating the chambers and toward the cholangiocytes was visualized by fluorescence microscopy after 24 hr. co-culture (top: 4x; bottom: 10x).

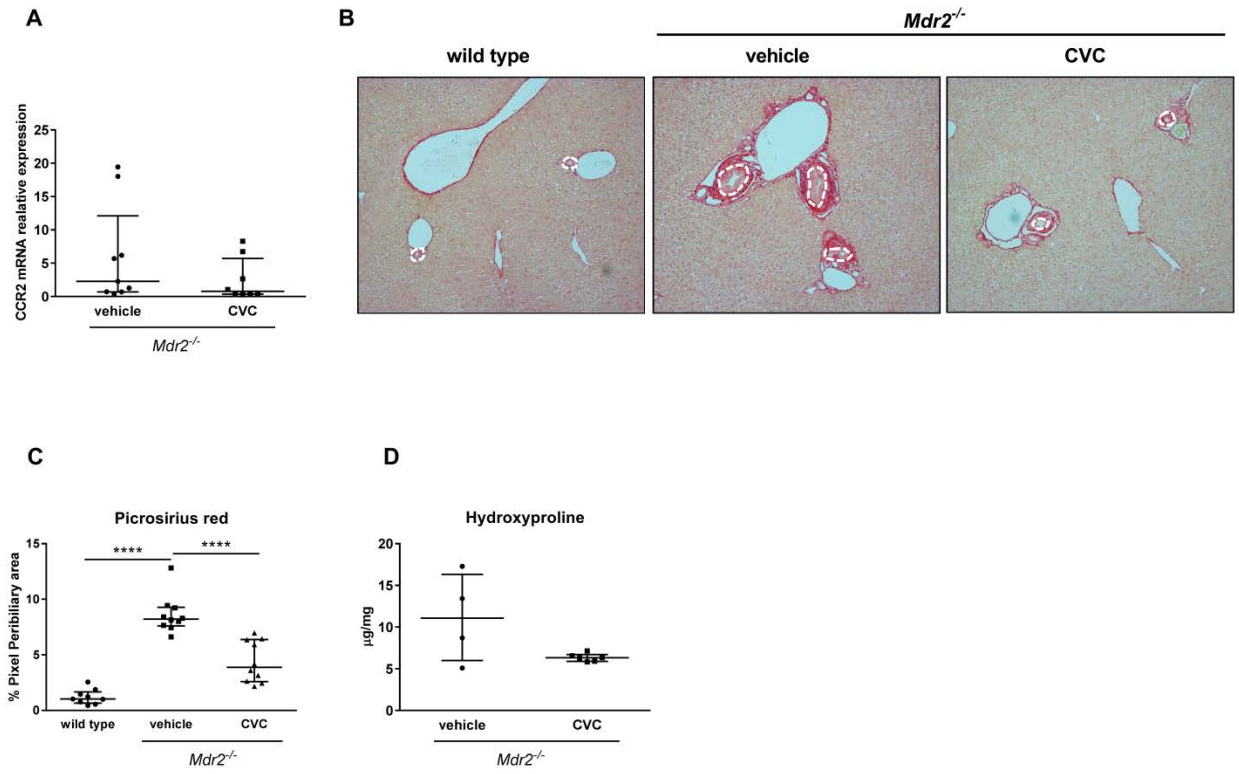

Fig. S5. CVC treatment attenuated liver fibrosis in Mdr2-/- mice. Sixty-day old C57BL/6.*Mdr2*$^{-/-}$ mice were treated with CVC as described in Materials and Methods (n=10 per group). **(A)** Monocyte-derived macrophage infiltration measured by *Ccr2* gene expression in whole livers vehicle- or CVC-treated mice by qPCR. *Ccr2* expression was normalized to HPRT levels (vehicle: n=9; CVC: n=8). **(B)** Picrosirius red staining of C57BL/6 wild-type, vehicle- and CVC-treated C57BL/6.*Mdr2*$^{-/-}$ mouse livers. **(C)** Quantification of picrosirius red positive peribiliary areas (wild type: n=9; vehicle: n=10; CVC: n=10). **(D)** Measurement of hydroxyproline content of whole livers (vehicle: n=4; CVC: n=10). **p<0.005

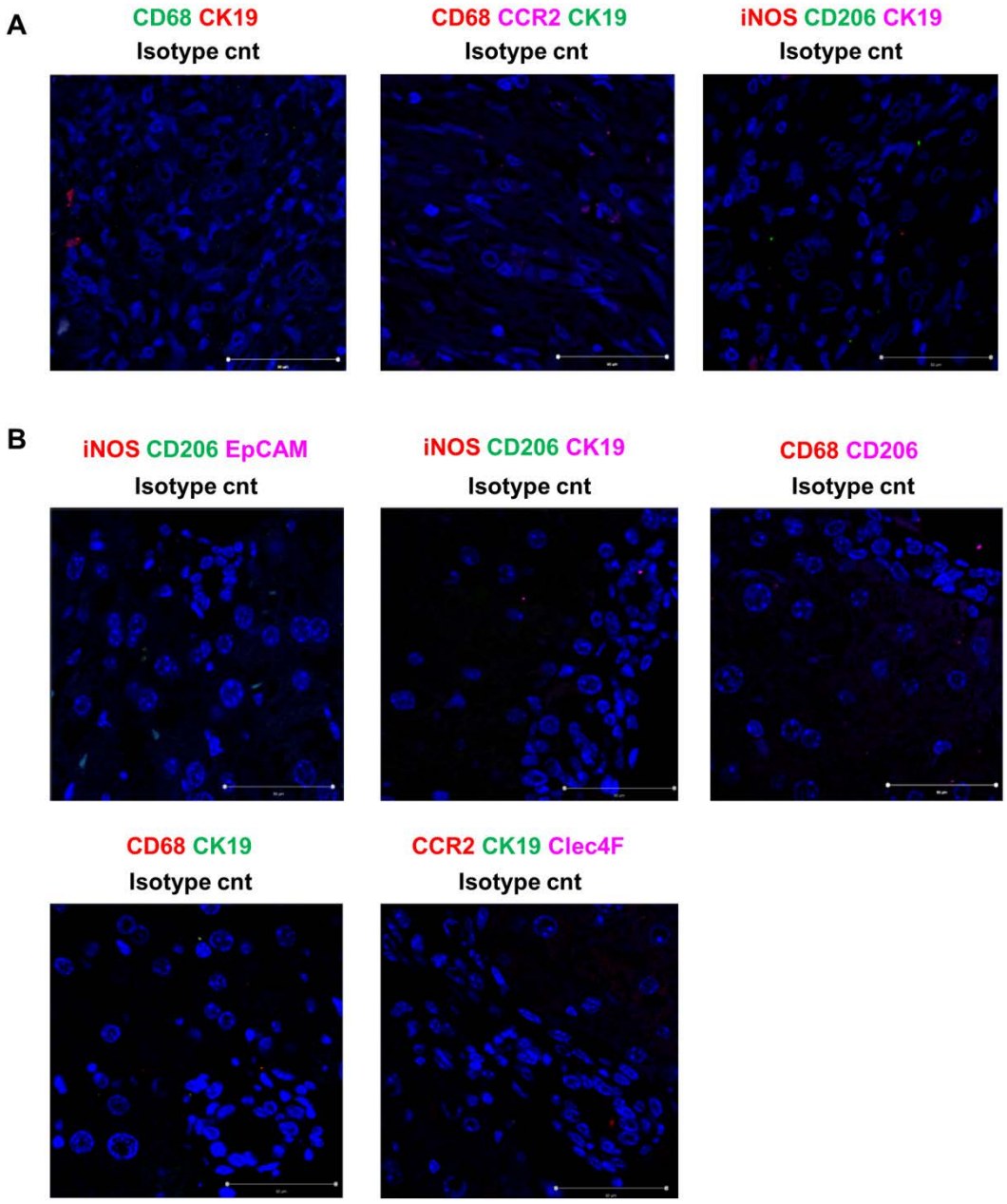

Fig. S6. Isotype controls for immunofluorescence. Normal IgG (isotype controls) used as negative controls in co-immunofluorescence on (A) human and (B) mouse liver tissue. Isotype controls were used at the same concentrations as their respective primary antibodies.

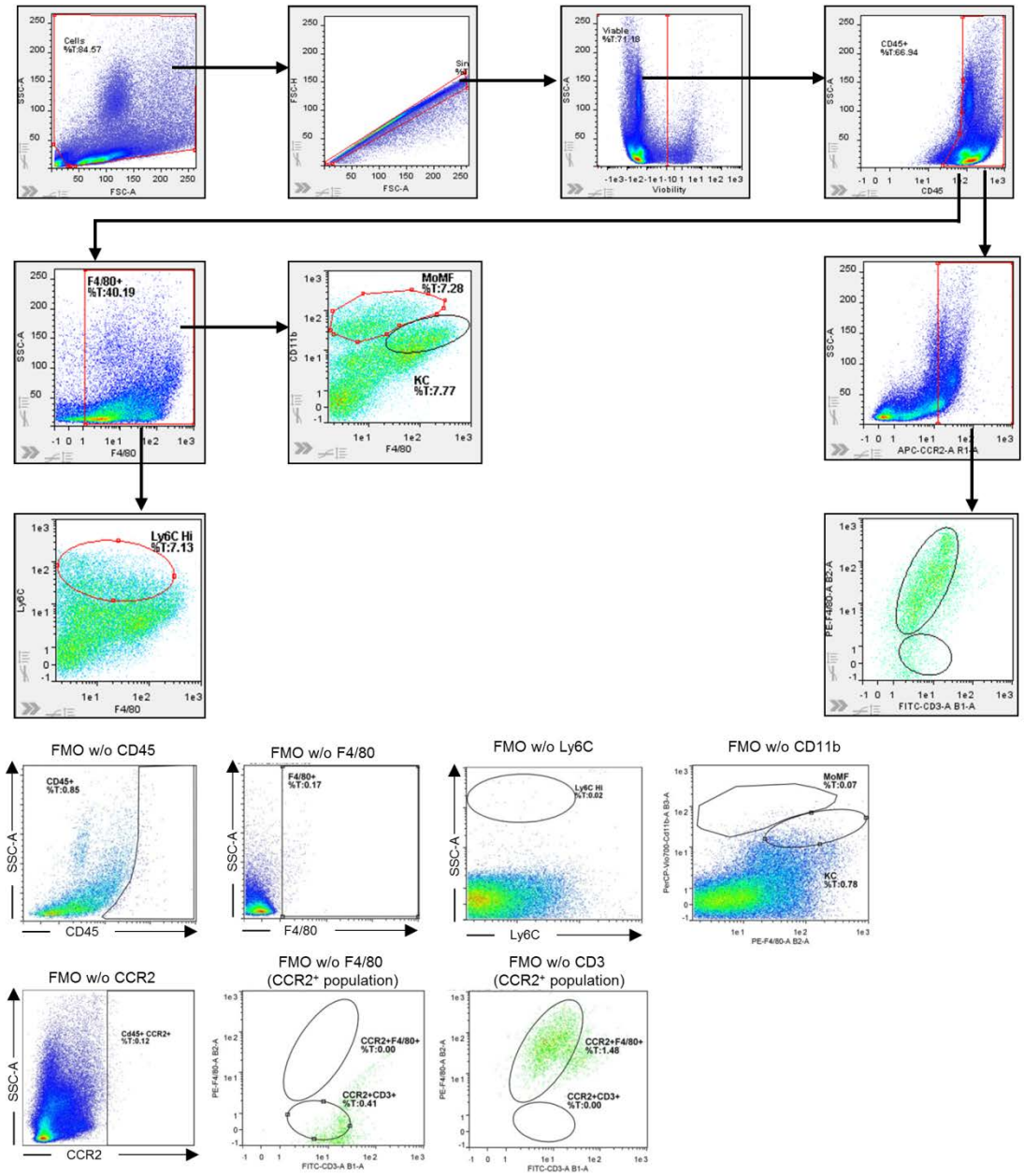

Fig. S7. Flow cytometry gating strategies and gating controls (FMO) for liver macrophages. Representative flow cytometric plots.

.

Table S1. Cell distribution of genes ≥ 2 fold upregulated in livers of BV6-injected vs. saline-injected mice

Gene ID	Fold change	P value	Cell distribution
Il1r2	9.92	0.0072	B cells, Mononuclear phagocytes, Neutrophils, T cells, Other
Ccl2	7.62	0.0067	Monocytes, Macrophages, Kupffer cells
Cd14	6.65	0.0007	Macrophages, Monocytes, Neutrophils, Other
Plaur	5.97	0.0001	Macrophages, Monocytes
Abcb1a	4.35	0.0060	Ubiquitous
Il1r1	4.22	0.0433	Monocytes, T cells, Other
Itgam	4.13	0.0047	Eosinophils, Hepatic Stellate Cells, Leukocytes, Lymphocytes, Macrophages, Monocytes, Neutrophils, Other
Fkbp5	4.11	0.0137	T and B cells, Monocytes, Bone marrow-derived Macrophages, Dendritic cells
Clec4e	4.00	0.0110	Dendritic cells, Macrophages
Ccl6	3.97	0.0004	Macrophages, Neutrophils (mouse only)
Irak3	3.70	0.0018	Monocyte, Macrophages, Epithelial cells
Cd24a	3.54	0.0180	B cells, Neutrophils
Runx1	3.46	0.0001	B cells, Dendritic cells, Macrophages, Monocytes, T cells, Other
Cd244	3.45	0.0048	Basophils, Eosinophils, Cd4+, Cd8+, NK cells, Monocytes
Defb1	3.32	0.0103	Dendritic cells, Macrophages, Monocytes, Other
Clec5a	3.22	0.0050	Macrophages, Monocytes
Cxcr4	3.18	0.0133	B cells, HSC, Lymphocytes, Macrophages, T cells, Other
Ccl3	3.11	0.0025	B cells, Macrophages, Monocytes, T cells
Marco	3.08	0.0043	Kupffer cells, Macrophages, Monocytes, Other
Il1rn	3.00	0.0390	Macrophages, T cells
Trem2	3.00	0.0110	NK cells, Myeloid cells, Other
Cxcr2	2.80	0.0056	Basophils, Granulocytes, Lymphocytes, Monocytes, Macrophages, NK cells, Mast cells, Neutrophils, UVEC
Vcam1	2.78	0.0019	Multiple cell types, Mast cells, UVEC, Other
Cd163	2.77	0.0093	Macrophages, Monocytes, Other
Tgfb2	2.76	0.0368	Multiple cell types
Cx3cl1	2.66	0.0218	Cholangiocytes, Dendritic cells, Liver epithelial cells, Other
Bst1	2.65	0.0353	Granulocytes, Macrophages, Monocytes, Mast cells, Neutrophils, UVEC, Other
Hamp	2.65	0.0131	Macrophages, Hepatocytes, Enterocytes
Cdkn1a	2.55	0.0010	B cells, T cells, Hematopoietic stem cells, Other
Cx3cr1	2.50	0.0358	Dendritic cells, Lymphocytes, Monocytes, Neutrophils, T cells, Other
Icam1	2.48	0.0013	Eosinophils, Lymphocytes, Neutrophils, T cells, Other
Tnfaip6	2.44	0.0441	Mesenchymal stem/stromal cells, PBMC, Neutrophils, Chondrocytes
Lilrb4	2.41	0.0019	B cells, Dendritic cells, Macrophages, Monocytes, NK cells, Other
Relb	2.35	0.0070	B cells, Macrophages, Monocytes, T cells, Other
Il1rl2	2.34	0.0015	Skin keratinocytes
Card9	2.28	0.0049	Granulocytes, Monocytes, T cells, Dendritic cells, Neutrophils
Nfkbiz	2.27	0.0055	Ubiquitous
Tlr2	2.27	0.0278	Monocytes; Other
Il6ra	2.25	0.0304	Ubiquitous
Itgb2	2.24	0.0021	Lymphocytes, Monocytes, Neutrophils, Other
Fcgr3	2.19	0.0021	Neutrophils, Keratinocytes
Nfkbia	2.18	0.0223	Neutrophils, T cells

Table S1. Cell distribution of genes ≥ 2 fold upregulated in livers of BV6-injected vs. saline-injected mice [cont.]

Gene ID	Fold change	P value	Cell distribution
Cd44	2.15	0.0231	Ubiquitous
Nfkb2	2.13	0.0113	Ubiquitous
Pdgfb	2.12	0.0103	Macrophages, Other
Il33	2.10	0.0071	Endothelial cells, Epithelial cells, Fibroblasts, Lymphocytes
Cul9	2.09	0.0007	Ubiquitous
Ikbke	2.08	0.0124	B cells, T cell, Other
Ncf4	2.08	0.0142	B cells, Basophils, Eosinophils, Mast cells, Monocytes, Neutrophils, Other
Lilrb3	2.06	0.0001	B cells, Dendritic cells, Eosinophils, Monocytes, NK cells, Other
Il18r1	2.04	0.0014	NK cells, T cells, Eosinophils, Dendritic cells
Plau	2.02	0.0414	Multiple cell types
Csf3r	2.02	0.0399	B cells, Granulocytes, Lymphocytes, Monocytes, Neutrophils, T cells, platelets
Cmklr1	2.01	0.0046	Multiple cell types
Itga4	2.01	0.0021	Hepatic Stellate Cells, Mast cell, Other

Table S2. Cell distribution of genes ≥ 2 fold upregulated in livers of C57Bl6.*Mdr2*$^{-/-}$ vs. wild-type C57Bl6 mice

Gene ID	Fold change	P value	Cell distribution
Il1rn	4.8	0.000204	Macrophages, T cells
Blnk	4.6	0.00033	B cells
Ccr2	4.3	0.00013	Macrophages, Monocytes, B cells, CD4+ Lymphocytes, Dendritic cells, Eosinophils, NK cells, Platelets, Kupffer cells
Slamf7	4.0	0.000521	B cells, CD4+ Lymphocytes, CD8+ Lymphocytes, Dendritic cells, NK cells
Cybb	4.0	0.000012	Macrophages, Monocytes, Neutrophils
Il17rb	3.8	0.000343	Lymphocytes, T cells, CD4+, Th2, iNKT
Cx3cr1	3.6	0.000543	Dendritic cells, Lymphocytes, Monocytes, Neutrophils, T cells , Other
Hamp	3.5	0.002333	Macrophages, Hepatocytes, Enterocytes
Ciita	3.1	0.00012	Macrophages, B cells, Dendritic cells
Src	3.1	0.000125	Ubiquitous
H2-Eb1	2.9	0.000564	B cells, Granulocytes, Monocytes, T cells
Trem2	2.8	0.004295	Lymphocytes
Thy1	2.8	0.000441	Endothelial cells, Lymphocytes, Monocytes, Neutrophils
Clec5a	2.7	0.002982	Macrophages, Monocytes
Itgax	2.7	0.002245	B cells, Hematopoietic stem cells, Lymphocytes, Macrophages, Monocytes, Neutrophils, Platelets, T cells
H2-Aa	2.5	0.001431	Dendritic cells, Macrophages, B cells, Endothelial cells, Epithelial cells
Pdgfb	2.4	0.000279	Macrophages, Other
Ltb	2.4	0.000783	Dendritic cells, Lymphocytes, Monocytes, Plasma cells, Thymocytes
H2-Ab1	2.4	0.00079	Dendritic cells, Macrophages, B cells, Endothelial cells, Epithelial cells
Cul9	2.3	2.35E-05	Ubiquitous
Tgfb2	2.3	0.000398	Multiple cell types
Cd9	2.3	0.003807	B cells, Monocytes, Platelets
Pdgfrb	2.2	0.000101	Endothelial cells, Decidual cells, Fibroblasts
Tlr1	2.2	0.002578	Monocytes, Polymorphonuclear leukocytes, T and B cells, NK cells
Cd74	2.1	0.001262	Dendritic cells, Macrophages, B cells, Endothelial cells, Epithelial cells
Clu	2.0	0.000955	PBMC, Platelets, Monocytes, B cells, NK cells

References

[1] Grubman SA, Perrone RD, Lee DW, Murray SL, Rogers LC, Wolkoff LI, et al. Regulation of intracellular pH by immortalized human intrahepatic biliary epithelial cell lines. Am J Physiol 1994;266(6 Pt 1): G1060-1070.

[2] Joplin R, Strain AJ, Neuberger JM. Immuno-isolation and culture of biliary epithelial cells from normal human liver. In Vitro Cell Dev Biol 1989;25(12): 1189-1192.

[3] Banales JM, Saez E, Uriz M, Sarvide S, Urribarri AD, Splinter P, et al. Up-regulation of microRNA 506 leads to decreased Cl-/HCO3- anion exchanger 2 expression in biliary epithelium of patients with primary biliary cirrhosis. Hepatology 2012;56(2): 687-697.

[4] Tabibian JH, Trussoni CE, O'Hara SP, Splinter PL, Heimbach JK, LaRusso NF. Characterization of cultured cholangiocytes isolated from livers of patients with primary sclerosing cholangitis. Lab Invest 2014;94(10): 1126-1133.

[5] Hirsova P, Ibrahim SH, Krishnan A, Verma VK, Bronk SF, Werneburg NW, et al. Lipid-Induced Signaling Causes Release of Inflammatory Extracellular Vesicles From Hepatocytes. Gastroenterology 2016;150(4): 956-967.

[6] Guicciardi ME, Krishnan A, Bronk SF, Hirsova P, Griffith TS, Gores GJ. Biliary tract instillation of a SMAC mimetic induces TRAIL-dependent acute sclerosing cholangitis-like injury in mice. Cell Death Dis 2017;8(1): e2535.

[7] Krishnan A, Li X, Kao WY, Viker K, Butters K, Masuoka H, et al. Lumican, an extracellular matrix proteoglycan, is a novel requisite for hepatic fibrosis. Lab Invest 2012;92(12): 1712-1725.

[8] Haque A, Gheibi P, Stybayeva G, Gao Y, Torok N, Revzin A. Ductular reaction-on-a-chip: Microfluidic co-cultures to study stem cell fate selection during liver injury. Sci Rep 2016;6: 36077.

[9] Yamaguchi K, Yang L, McCall S, Huang J, Yu XX, Pandey SK, et al. Inhibiting triglyceride synthesis improves hepatic steatosis but exacerbates liver damage and fibrosis in obese mice with nonalcoholic steatohepatitis. Hepatology 2007;45(6): 1366-1374.